Polymer Engineering & Science

WILEY | spe INSPIRING PLASTICS PROFESSIONALS

RESEARCH ARTICLE OPEN ACCESS

Rheological Characterization and Multi-Regime Viscosity Modeling of Diluted Polyethylene Mixtures

Johannes Krug[1,2] | Ernst Georg Viehböck[2,3] | Alexander Hammer[2] | Ursula Steiner[2] | Christof Murnig[4] | Martin Reichel[4] | Christian Paulik[3,5] | Gerald Berger-Weber[2]

[1]Pro2Future GmbH, Linz, Austria | [2]Institute of Polymer Processing and Digital Transformation, Johannes Kepler University Linz, Linz, Austria | [3]Competence Center CHASE GmbH, Linz, Austria | [4]GAW Technologies GmbH, Graz, Austria | [5]Institute of Chemical Technology of Organic Materials, Johannes Kepler University Linz, Linz, Austria

Correspondence: Ernst Georg Viehböck (ernst.viehboeck@chasecenter.at)

Received: 6 March 2026 | **Revised:** 10 April 2026 | **Accepted:** 12 April 2026

Keywords: complex viscosity | Cox–Merz rule | polymer solutions | shift factors | steady-shear flow | viscosity modeling

ABSTRACT

Solvent-assisted recycling processes, such as the CreaSolv-technology, represent a critical pathway for closing the loop on complex polyolefin waste streams. However, the optimization of unit operations, from dissolution to devolatilization, is frequently impeded by the lack of constitutive models capable of describing the rheological behavior of recycled polymers across the entire concentration regime. This study investigates the viscoelastic properties of low-density polyethylene (PE-LD), a branched and multimodal polymer, dissolved in a specialty solvent specific to the recycling process. Systematic steady-shear and oscillatory measurements were conducted to map the flow behavior from the dilute solution to the entangled melt (0 to 100 m% polymer content). To bridge the gap between theoretical fidelity and industrial applicability, a semiempirical modeling framework based on a combination of time–concentration superposition (TCS) and time–temperature superposition (TTS) was developed. The derived model unifies the dependencies of temperature, shear rate, and diluent concentration, capturing the transition from Newtonian plateaus to pronounced shear-thinning regions. Despite the complexity of the polymer-diluent mixture, the model predicts the viscosity over nine decades with a mean relative error (MRE) of less than 12%. These findings provide a robust, computation-efficient tool for the design and scale-up of solvent-assisted recycling equipment.

1 | Introduction

Solvent-assisted recycling processes, particularly dissolution-precipitation techniques, have emerged as a pivotal pathway for recovering high-quality polyolefins from complex waste streams where mechanical recycling reaches its limits [1, 2]. The efficiency of the associated unit operations, ranging from dissolution and pumping to devolatilization, is intrinsically governed by the rheological behavior of the polymer solution. This dependency arises because viscosity correlates with viscous dissipation, which directly dictates energy consumption during transport, processing, and mixing, while devolatilization rates are fundamentally limited by the mass transfer of the volatile species, a process that exhibits a strong reciprocal correlation with the mixture's macroscopic viscosity [3]. In these processes, the viscosity varies drastically, transitioning from the low-viscosity Newtonian plateau of the pure solvent to the high-viscosity Newtonian plateau and subsequent pronounced shear-thinning behavior of the pure polymer melt. Consequently, the optimization of such industrial applications requires robust constitutive models capable of describing the non-Newtonian viscosity continuously across the entire concentration regime.

From a molecular perspective, the dynamics of entangled polymer systems can be modeled by the tube model and reptation

Highlights

- Systematic rheological characterization of PE-LD diluted with a specialty solvent from 0 to 100 m%.
- Validation of thermorheological and concentration-rheological simplicity for highly branched polymer-diluent mixtures.
- Development of a semiempirical multi-regime viscosity model integrating Carreau–Yasuda, TTS, and TCS principles.
- Accurate prediction of steady-shear viscosity over nine decades with a mean relative error below 12%.
- Computationally efficient modeling framework to aid the design and scale-up of solvent-assisted recycling unit operations.

theory, where the polymer chain is confined within a virtual tube defined by topological constraints [4]. The incorporation of a diluent induces profound alterations in these dynamics, primarily through two concurrent mechanisms: the dilution of the entanglement network, effectively widening the tube, and the reduction of the monomeric friction coefficient due to increased fractional free volume [5]. While theoretical scaling concepts for good solvents suggest that the zero-shear viscosity follows a power law $\eta_0 \sim c^{\alpha}$ (with α typically ranging between 3.4 and 4.5 depending on the regime), accurately describing the transition from semi-dilute to concentrated regimes for polydisperse industrial polymers remains a challenge [6, 7].

To consolidate experimental data across these distinct regimes, the classical time–temperature superposition (TTS) principle is extended to include concentration effects, a methodology known as time–concentration superposition (TCS) [8]. This approach postulates that viscoelastic spectra obtained at various concentrations can be superimposed onto a master curve of the reference melt via specific horizontal (a_c) and vertical (b_c) shift factors.

The vertical shift factor, b_c, quantifies the dilution of the entanglement network density. Consistent with the binary contact model, b_c is generally found to scale with the square of the polymer weight fraction at least for concentrated solutions of polystyrene and other model polymers [9, 10] or polyethylene with *n*-alkanes [11]. In contrast, the horizontal shift factor a_c, which describes the acceleration of relaxation times, is influenced by both the disentanglement and the change in local friction. This dependence is successfully modeled using free volume concepts, such as the generalized Doolittle equation [12], or hybrid models that explicitly separate hydrodynamic scaling from thermodynamic free volume effects using equations of state (EOS) like Sanchez–Lacombe [13, 14].

While these theoretical frameworks provide a rigorous basis for linear model polymers, their application to PE-LD is nontrivial due to the presence of long-chain branching (LCB). LCB introduces thermorheological complexity, potentially disrupting simple superposition principles due to the distinct temperature sensitivities of backbone and branch relaxation processes [15, 16]. Furthermore, industrial recycling requires predictive tools that avoid the heavy computational burden of explicit EOS parameters, which are often unavailable for complex postconsumer waste streams.

This study addresses these challenges by applying a combined TTS and TCS methodology to establish a semiempirical model for a PE-LD/solvent system associated with the CreaSolv-technology. The scientific novelty of this work lies in the validation of concentration-rheological simplicity for a non-model, highly branched and multimodal polyolefin across the entire concentration regime (0 to 100 m%). From a practical perspective, by fitting the resulting master curves to a generalized Carreau–Yasuda model, we provide a robust and computationally efficient tool for the design and scale-up of solvent-assisted recycling unit operations. This framework enables the prediction of viscosity over nine decades, covering the drastic transitions from the dilute solvent to the entangled melt, which is critical for optimizing operations such as pumping, filtration, and devolatilization in circular economy processes.

2 | Experimental

2.1 | Materials

To systematically investigate the viscoelastic properties and viscosity reduction in polymer-solvent systems, a representative commercial polymer and a specific process solvent were selected.

The polymeric base material employed in this study was a PE-LD grade Lupolen 1800H (LyondellBasell Industries NV, Frankfurt, Germany) used for injection molding, blow molding, and film extrusion. This grade is characterized by a melt flow rate (MFR) of 1.5 g/10 min (measured at 190°C with a load of 2.16 kg).

As the diluent, a commercial solvent formulation associated with the CreaSolv-Process (CreaCycle GmbH, Grevenbroich, Germany) was utilized (abbreviated as CS). This solvent was specifically chosen due to its high compatibility with polyolefins and its demonstrated effectiveness in significantly reducing the viscosity of polyethylene melts, as detailed in previous investigations [17].

2.2 | Rheometry

All rheological measurements were conducted using a modular compact rheometer (MCR 302, Anton Paar GmbH, Graz, Austria). To accommodate the vast dynamic range of viscosity, spanning from the highly entangled polymer melt to the low-viscosity pure solvent, the experimental protocol was stratified into four distinct configurations utilizing different geometries and shear modes:

1. Pure polymer melt (0 wt% solvent): Small-amplitude oscillatory shear (SAOS) measurements were performed using a parallel-plate geometry (PP25).

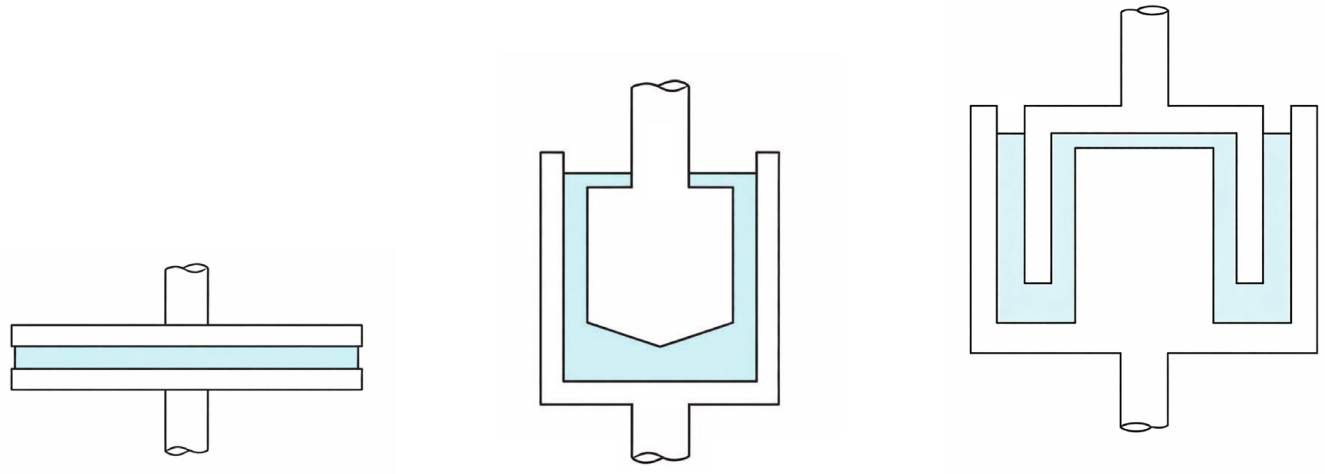

(a) Parallel-plate (PP25) (b) Concentric cylinder (CC27) (c) Double-gap (DG26.7)

FIGURE 1 | Schematic representations of the rheological geometries: (a) parallel-plate (PP25, $d = 25$ mm), (b) concentric cylinder (CC27, diameter of the measuring cup = 27 mm), and (c) double-gap (DG26.7, diameter of the measuring bob = 26.7 mm) for low-viscosity characterization.

2. Concentrated solutions (20–60 wt% solvent): SAOS measurements were conducted using a concentric cylinder setup (CC27), as depicted on Figure 1a.
3. Semi-dilute solutions (70–90 wt% solvent): Steady-shear flow tests (SFT) were employed using the concentric cylinder (Couette) geometry (CC27), as the low viscosity precluded accurate oscillatory testing within the instrument's torque resolution, as depicted on Figure 1b.
4. Pure solvent (100 wt%): SFT measurements were carried out using a double-gap geometry (DG26.7) to maximize the shear surface area for high-precision low-viscosity determination, as depicted on Figure 1c.

Prior to the main characterization in the oscillatory regime, amplitude sweeps were performed for all samples at each test temperature to determine the linear viscoelastic (LVE) limit. Based on these results, a constant strain amplitude within the linear range was selected for all subsequent dynamic tests to ensure a strain-independent material response.

Generally, for non-Newtonian fluids in rotational rheometry, the shear rate at the wall differs from the Newtonian calculation, necessitating the Weissenberg–Rabinowitsch correction. However, the employed geometry conforms to the ISO 3219 standard, which stipulates a narrow gap ratio of $\delta \leq 1.0847$. Under this condition, the shear rate distribution across the gap is sufficiently linear, and the approximation error remains negligible. Consequently, the explicit Weissenberg–Rabinowitsch correction was not applied for this setup [18].

Furthermore, to validate the data and exclude artifacts arising from wall slip, systematic tests were performed using a parallel-plate configuration with varying gap heights, following the method described by Yoshimura and Prud'homme [19]. The results exhibited no dependence of the measured viscosity on the gap setting, confirming that wall slip effects were negligible for the investigated systems.

2.3 | Sample Preparation

To ensure reproducibility and a consistent thermomechanical history, a standardized preparation protocol was established for all samples. The mixtures were prepared within the cup of the CC27 setup to avoid material loss during transfer. A constant total sample mass of 18 g was maintained for each specimen. The preparation sequence involved first loading the solid polymer granules into the cylinder, followed by the addition of the specific mass of liquid solvent, both determined via gravimetric analysis.

Homogenization of the polymer-diluent system was carried out directly at the target measurement temperature using a custom-fabricated U-shaped stirrer. The mixing process was continuously monitored via torque readings and continued until a constant equilibrium torque was reached, indicating the formation of a macroscopically homogeneous melt. To minimize solvent loss due to volatility at elevated temperatures, a solvent trap was utilized throughout the entire preparation and testing procedure.

Upon verification of homogeneity via the torque signal and supplementary manual mixing, the stirring element was removed. To minimize thermal gradients and prevent local cooling of the melt upon contact, the CC27 measuring cylinder was preheated to the test temperature prior to insertion. Immediately following insertion, the system was resealed with the solvent trap to prevent evaporation during the subsequent rheological measurements.

A schematic illustration of the sample preparation workflow is provided in Figure 2.

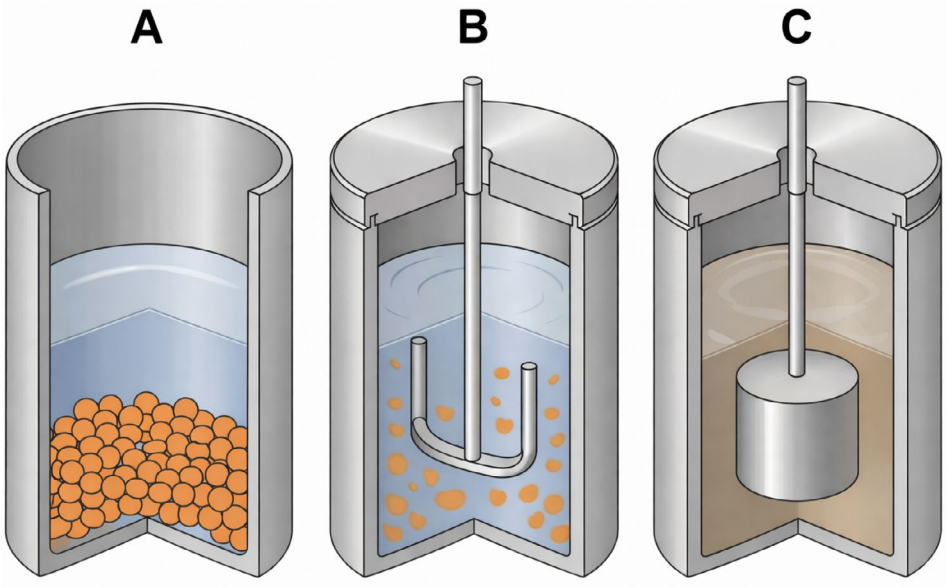

FIGURE 2 | Schematic overview of the employed methodology: (a) Loading of polymer granules and liquid solvent into the CC27 cylindrical cup; (b) homogenization of the mixture at the measurement temperature using a stirrer equipped with a solvent trap; (c) final setup with the measuring bob inserted into the homogenized melt (illustration generated via ChatGPT).

3 | Modeling

To describe the complex rheological behavior of the PE-LD/diluent system across the entire concentration range, a semiempirical modeling approach based on the Carreau–Yasuda model was extended. The primary objective was to capture the dependence of steady-shear viscosity (η) on shear rate ($\dot{\gamma}$), temperature (T), and polymer weight fraction (w_p).

3.1 | Shear Rate Dependence: The Carreau–Yasuda Model

The experimental data exhibited a characteristic transition from a Newtonian plateau at low shear rates to a shear-thinning regime at higher deformation rates. To capture this behavior across the entire range of shear rates, the Carreau–Yasuda model was selected [20, 21]. This model is widely preferred over the simple power-law model because it accurately describes the zero-shear viscosity, the power-law shear-thinning regime, and especially its transition [22, 23].

The dependence of the viscosity η on the shear rate $\dot{\gamma}$ is given by Equation (1):

$$\frac{\eta(\dot{\gamma}) - \eta_\infty}{\eta_0 - \eta_\infty} = \left[1 + (\lambda\dot{\gamma})^a\right]^{\frac{n-1}{a}}. \tag{1}$$

In this expression, η_0 represents the (theoretical) zero-shear viscosity, at low shear rates ($\dot{\gamma} \to 0$). The parameter η_∞ denotes the infinite-shear viscosity commonly assumed as 0 Pa s. The characteristic relaxation time λ determines the onset of shear-thinning; its reciprocal value ($1/\lambda$) marks the critical shear rate at which the fluid transitions from Newtonian to non-Newtonian behavior. The degree of shear-thinning is governed by the power-law index n (where $0 < n < 1$ for pseudoplastic fluids). Furthermore, the introduction of the dimensionless Yasuda parameter a allows for an adjustment of the curvature width in the transition region between the Newtonian plateau and the power-law zone [21]. This flexibility is particularly advantageous for polydisperse materials like the PE-LD used in this study, which typically exhibit a broader relaxation spectrum compared to monodisperse polymers.

3.2 | Temperature Dependence: TTS

The variation of rheological properties with temperature is intrinsically linked to the mobility of the polymer chains and the available free volume within the melt [8]. To account for these thermal effects and to consolidate the experimental viscosity and moduli data onto a single master curve, the TTS principle was applied. While the Williams–Landel–Ferry (WLF) equation is the standard approach for amorphous polymers in the vicinity of their glass transition temperature (T_g) [24], the polyethylene systems investigated in this study were processed at temperatures ranging from 140°C to 180°C. Since this experimental window is located far above the glass transition of PE ($T \gg T_g$ + 100 K), the nonlinear dependency characteristic of the WLF model becomes negligible.

Consequently, the temperature dependence of the temperature shift factor a_T is accurately described by the Arrhenius relationship, which assumes a constant activation energy for flow over the tested range [23, 25]. The shift factor relative to a reference temperature T_{ref} is defined in Equation (2):

$$a_T(T) = \exp\left[\frac{E_a}{R}\left(\frac{1}{T} - \frac{1}{T_{ref}}\right)\right] \tag{2}$$

In this expression, R denotes the universal gas constant, while T and T_{ref} represent the absolute measurement and reference temperatures, respectively. The flow activation energy, E_a, serves as a material-specific parameter that quantifies the sensitivity of

TABLE 1 | Optimized model parameters characterizing the Carreau–Yasuda fluid behavior, Arrhenius temperature dependence (TTS), and concentration scaling (TCS) for the PE-LD/CS system at the reference temperature of 140°C.

	Master curve (CY)				TTS	TCS				
Sample	η_0 (Pa s)	λ (s)	n (-)	a (-)	E_a (J/mol)	$\beta_{c,140}$ (-)	$\beta_{c,160}$ (-)	$\beta_{c,180}$ (-)	β_{conc} (-)	β_{dil} (-)
PE-LD/CS	44,695	14.3	0.476	0.598	49,288	9.30	9.01	8.41	1.99	2.68

the zero-shear viscosity to temperature variations [15]. By determining a_T experimentally, E_a was derived via linear regression of $\ln(a_T)$ versus $1/T$.

3.3 | Concentration Dependence: TCS

To describe the concentration-dependent viscosity $\eta(\phi)$ or $\eta(w_p)$ of polymer systems, the TCS principle is employed as a fundamental constitutive framework. Analogous to the TTS principle, TCS posits that variations in the polymer volume fraction ϕ induce a self-similar shift of the viscoelastic spectrum without altering the underlying relaxation mechanisms, provided the system remains within a consistent dynamic regime, such as the entangled state [7, 26]. Following the framework established by Schausberger and Ahrer, the global shift in steady-shear viscosity upon dilution is analytically decomposed into a vertical shift factor b_c, representing the concentration-dependent modulus, and a horizontal shift factor a_c, associated with the characteristic relaxation times [12].

While this methodology is well-established for linear polymers with a unimodal molecular weight distribution (MWD), its application to postconsumer recyclate streams necessitates the consideration of complex macromolecular architectures. Mechanical recycling invariably yields heterogeneous mixtures of various polymer grades, often characterized by LCB and broad, multimodal MWDs, which significantly alter the rheological response. To validate the industrial utility of the TCS paradigm for real-world recycling applications, this study evaluates the methodology using PE-LD. As a heavily branched polymer with a broad MWD, PE-LD serves as a representative model for the complex fractions dominating postconsumer flexible packaging waste [27].

The vertical shift factor b_c quantifies the dilution of the entanglement network density. For concentrated polymer solutions and melts, b_c typically follows a power-law scaling, a dependence theoretically substantiated and experimentally validated for various systems, including polyolefins and polystyrene diluted with oligomeric solvents [9, 10, 28]. In highly entangled systems, dynamic scaling arguments suggest a plateau modulus scaling of $G_N^0 \sim c^{2.29}$, aligning with the "blob" model for concentrated regimes in good solvents [26]. However, rheological analysis utilizing the van Gurp–Palmen (vGP) plot (phase angle δ vs. absolute complex modulus $|G^*|$) provides a robust, model-independent criterion for evaluating the necessity of b_c. The vGP plot serves as a definitive indicator of concentration-rheological simplicity. If the $\delta(|G^*|)$ profiles of the diluted species superimpose onto the reference curve of the neat polymer without requiring a prior density or concentration correction, the system is considered rheologically simple with respect to dilution. Under such conditions, the vertical shift factor mathematically reduces to unity ($b_c = 1$), implying that the introduction of the solvent strictly accelerates the global relaxation dynamics ($a_c < 1$) while leaving the fundamental magnitude of the dynamic moduli unaffected.

The horizontal shift factor a_c represents the acceleration of segmental relaxation processes upon dilution, primarily governed by increases in the fractional free volume f_c. Schausberger and Ahrer modeled this dependence using a generalized Doolittle equation, treating the free volume of the mixture as a linear function of the additive concentration [12]. While thermodynamic approaches utilizing EOS, such as the Sanchez–Lacombe theory, offer high theoretical fidelity for predicting free volume in systems involving supercritical fluids, their industrial applicability is often computationally prohibitive or limited by unknown interaction parameters [13, 14, 17, 29].

Recent advancements demonstrate that a_c and b_c can be effectively described by distinct power-law scalings ($a_c \sim c^{\alpha}$, $b_c \sim c^{\beta}$) capable of capturing critical regime transitions, such as the crossover from the semi-dilute unentangled regime to the fully entangled regime [7, 26]. To establish a robust diagnostic model that remains independent of explicit thermodynamic parameters or precise MWD factors, data often unavailable for industrial recycle streams, this study adopts a regime-dependent empirical scaling approach.

Based on this framework, the concentration-dependent shift factors are formulated as functions of the polymer weight fraction w_p. The model accounts for the acceleration of relaxation dynamics through a combined phenomenological approach. The horizontal shift factor a_c incorporates both power-law and exponential contributions to capture free volume effects and dynamic scaling, while the vertical shift factor b_c is defined by a power-law dependence. To accurately represent the distinct rheological responses across different concentration intervals, the scaling exponents are treated as regime-dependent parameters:

$$a_c(w_p, T) = w_p^{\beta} \exp\left(-\beta_c(T) \cdot (1 - w_p)\right) \tag{3}$$

$$b_c(w_p) = w_p^{\alpha} \tag{4}$$

Here, the exponents α and β assume distinct values depending on whether the system is situated within the semi-dilute or the concentrated entangled regime. Crucially, the parameter $\beta_c(T)$ represents a strictly temperature-dependent scaling exponent. As validated by the global optimization (see Table 1), $\beta_c(T)$ accounts for the varying efficiency of solvent-induced free volume generation at different isotherms and remains entirely independent of the polymer concentration w_p.

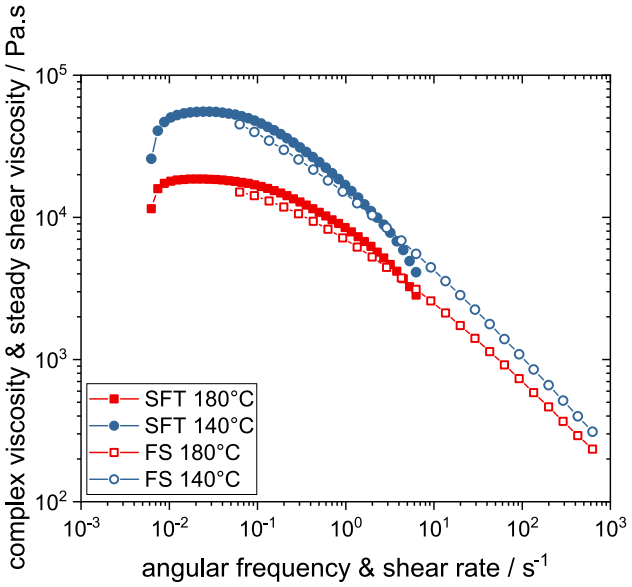

(a) Validation of the Cox-Merz rule at 0 % diluent concentration.

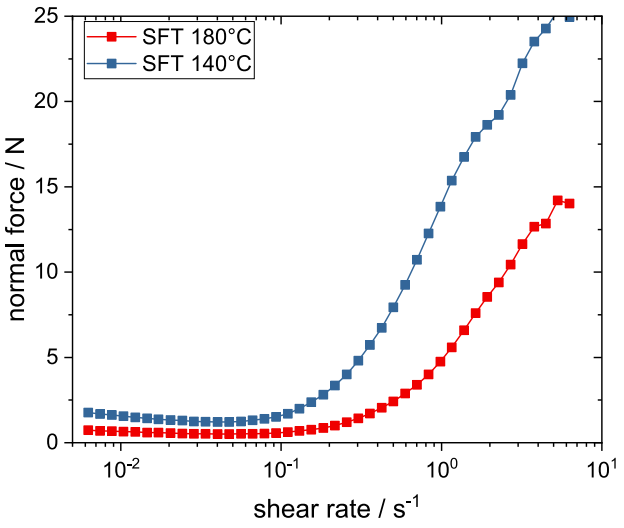

(b) Normal force evolution during steady-shear.

FIGURE 3 | Definition of the valid rheological measurement window for the undiluted polymer. (a) Superposition of complex and steady-shear viscosity confirming the Cox–Merz rule at the boundary concentrations. (b) Normal force monitoring to identify the onset of the Weissenberg effect, establishing the valid shear rate limit ($\dot{\gamma} \leq 0.1\ s^{-1}$) at low dilution.

4 | Results and Discussion

4.1 | LVE Limits and Data Validation

To ensure that the dynamic oscillatory measurements reflect the equilibrium structure of the polymer network, amplitude sweeps were conducted to define the LVE regime. For the PE-LD/diluent mixtures, strain amplitudes of $\gamma_0 \leq 10\,\%$ were found to remain well within the LVE region across the temperature range of 140°C–180°C. Consistent with rheological theory for concentrated solutions, the critical strain amplitude for the onset of nonlinearity shifted to higher values with increasing diluent concentration. This behavior is attributed to the reduction in entanglement density and the associated decrease in the plateau modulus G_N^0, which generally allows for larger deformations before the network structure is disrupted.

Prior to evaluating the concentration-dependent viscosity reduction, the fundamental rheological boundary conditions were established using the neat polymer melt (0 wt% diluent) across the investigated temperature range. The applicability of the empirical Cox–Merz rule, which equates the magnitude of the complex viscosity $|\eta^*(\omega)|$ with the steady-shear viscosity $\eta(\dot{\gamma})$ when the angular frequency ω equals the shear rate $\dot{\gamma}$ [15, 30, 31], was explicitly validated for this system, as shown in Figure 3a. At low diluent concentrations, SFT are frequently complicated by the Weissenberg effect, which generates significant normal forces acting on the plate geometry. To ensure data integrity, the normal force was continuously monitored during the measurements (Figure 3b). These measurements were conducted using the integrated sensor within the air bearing-supported motor head of the MCR 302 rheometer, which records the axial thrust exerted by the sample directly on the actuator side. The onset of a sharp increase in this signal served as a diagnostic physical criterion to determine the upper limit of stable laminar flow before the onset of edge fracture or radial sample ejection from the measuring gap. Consequently, steady-shear measurements for these highly entangled states were considered valid only up to a critical shear rate of $\dot{\gamma} = 0.1\ s^{-1}$. Once this valid experimental window was defined, the analysis was systematically extended to the concentration-dependent regimes.

Comparison of the oscillatory and steady-shear flow data demonstrated excellent agreement at both the lower bound (0% diluent) and the upper bound of the oscillatory experimental window (60% diluent). Therefore, the Cox–Merz rule is considered valid across the entire investigated concentration range. It should be noted that at diluent concentrations exceeding 60%, the severe viscosity reduction resulted in torque signals falling below the resolution limit for reliable frequency sweeps (FS); in these semi-dilute regimes, structural characterization relied exclusively on SFT experiments [22].

To rigorously validate the fundamental fluid mechanical assumption of the no-slip boundary condition, a systematic varying gap analysis was executed in accordance with the established methodology of Yoshimura and Prud'homme. Oscillatory shear measurements were performed utilizing a parallel-plate configuration at discrete gap heights (specifically 0.6 and 0.95 mm) to explicitly identify potential apparent slip layers. As illustrated for a representative system at a constant concentration and intermediate temperature in Figure 4, the magnitude of the complex viscosity demonstrates strict superposition irrespective of the applied gap separation. This geometric invariance of the viscoelastic material functions provides evidence for the suppression of macroscopic wall slip phenomena, thereby guaranteeing that the acquired data exclusively reflect the true rheological bulk properties of the investigated systems [19, 32].

4.2 | Compositional Stability

A critical challenge in the rheometry of polymer solutions at elevated temperatures is the potential desorption or evaporation of the volatile diluent during measurement [33, 34]. To assess the compositional stability of the samples, a time-dependent validity check was implemented by remeasuring the initial viscosity point after the completion of the frequency sweep. These verification steps consistently yielded deviations of less than 5%, confirming that solvent evaporation was negligible and that the diluent concentration remained effectively constant throughout the duration of the rheological experiments.

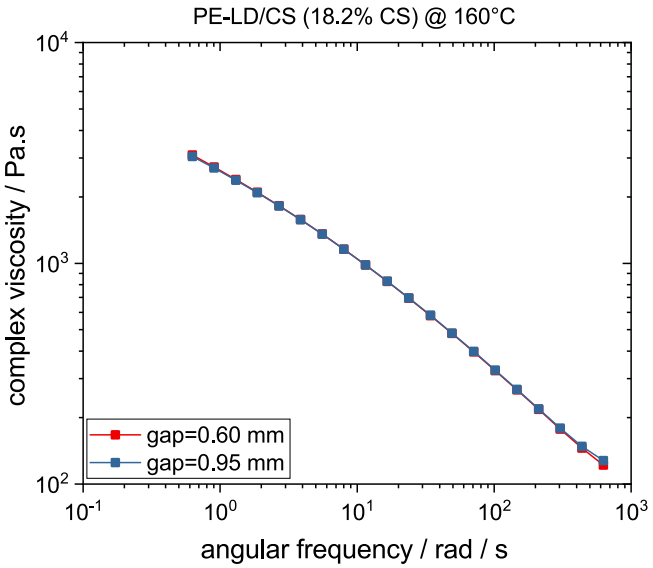

FIGURE 4 | Validation of the no-slip boundary condition via a varying gap study. The magnitude of the complex viscosity $|\eta^*|$ is plotted as a function of angular frequency ω for varying gap heights. The strict superposition of the data confirms the absence of apparent wall slip.

4.3 | Time–Temperature Superposition

The validity of the TTS principle was assessed using van Gurp–Palmen (vGP) plots (phase angle δ vs. complex modulus $|G^*|$). While PE-LD typically exhibits thermorheological complexity due to the presence of LCB [15, 35], the superposed data for both the neat polymer and the solutions show good agreement, as illustrated in Figure 5. This confirms that, within the experimental window (excluding the high-frequency regime), the relaxation mechanisms can be approximated as thermorheologically simple for diluent concentrations up to 50 m%.

The temperature dependence of a_T follows an Arrhenius relationship as the measurement temperatures are significantly above the glass transition temperature ($T \gg T_g + 100$ K) [24]:

$$\ln(a_T) = \frac{E_a}{R}\left(\frac{1}{T} - \frac{1}{T_{ref}}\right) \tag{5}$$

where E_a is the flow activation energy and R is the universal gas constant. Figure 6 shows the Arrhenius plot of $\ln(a_T)$ versus the

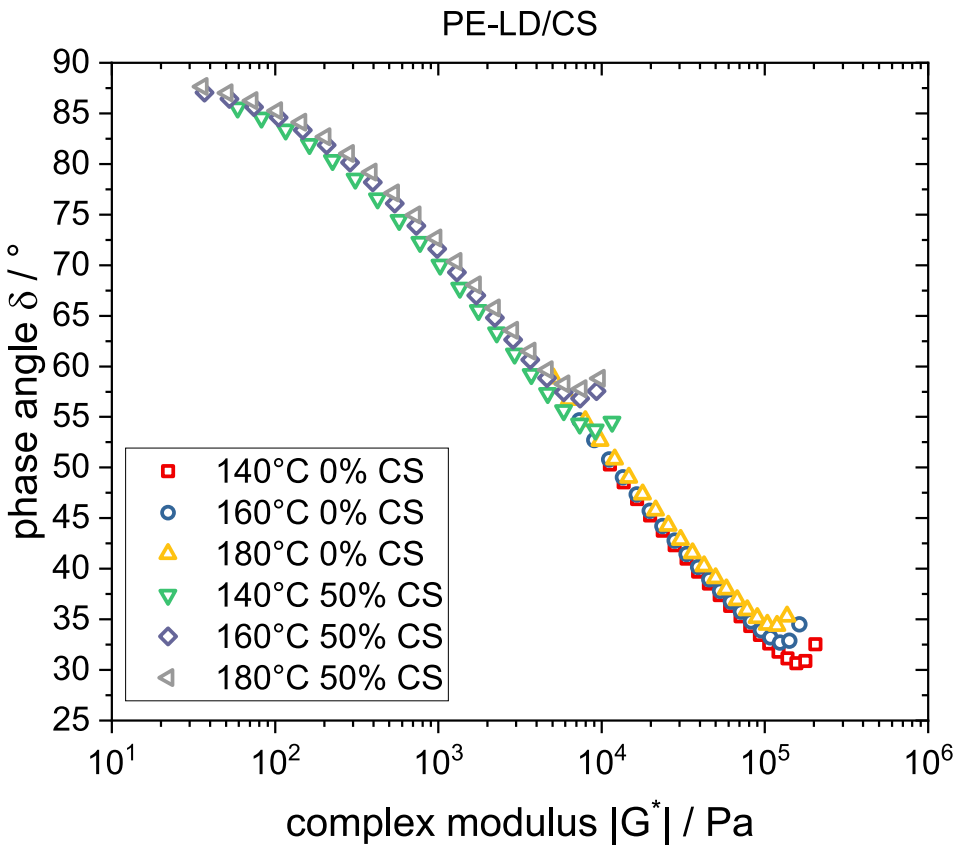

FIGURE 5 | van Gurp–Palmen plot of PE-LD/CS systems at varying temperatures and concentrations. The smooth superposition of the curves confirms thermorheological simplicity across the investigated experimental window.

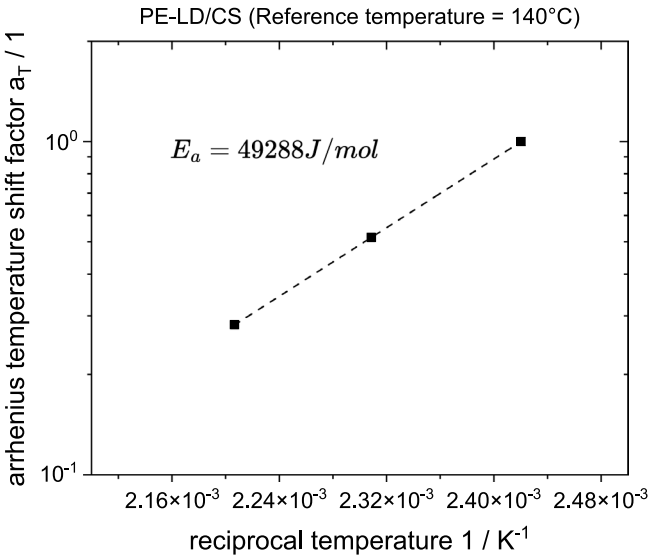

FIGURE 6 | Arrhenius plot of the temperature shift factors a_T.

inverse absolute temperature $1/T$. The linear regression yields an activation energy of $E_a = 49,288$ J/mol for the PE-LD/CS system, consistent with values reported for branched polyethylene architectures [36].

4.4 | Time–Concentration Superposition

Analogous to the validation of TTS, the applicability of the TCS principle was assessed using van Gurp–Palmen representations. Figure 7 presents the vGP plots for the PE-LD/CS systems across all investigated temperatures and concentrations. The data exhibit excellent superposition, confirming that the material behaves as concentration-rheologically simple [26].

To further substantiate this finding, the LVE spectra were shifted onto a reference master curve. Figure 8 depicts the superposed (a) storage modulus G' and (b) loss modulus G'' as a function of the reduced frequency $a_c\omega$. The successful collapse of the data points from various concentrations (20 to 50 m% solvent) onto the reference curves of the neat polymer melt confirms that the shape of the relaxation spectrum remains invariant upon dilution. Notably, this coalescence is achieved without applying a vertical density correction factor (b_c), as the vGP plots already indicated that the vertical shift is mathematically equivalent to unity ($b_c = 1$). Consequently, the observed reduction in complex viscosity is attributed exclusively to the horizontal shift factor a_c, indicating that dilution primarily accelerates the global relaxation dynamics without significantly altering the modulus scale in this concentrated regime.

4.5 | Modeling Framework and Parameter Identification

The primary objective of this study was to establish a robust phenomenological framework capable of predicting the steady-shear viscosity reduction induced by dilution with high computational efficiency. While rigorous theoretical approaches, such as those combining the Sanchez–Lacombe Equation of State (SL-EOS) with free volume theory, offer substantial predictive accuracy, their application is frequently hindered by the requirement for extensive thermodynamic parameters. These are often inaccessible for complex industrial recyclate streams and are typically restricted to the concentrated regime. Consequently, a semiempirical modeling framework was adopted. Although simplified to exclude explicit EOS parameters, the model retains a strict physical basis by adhering to the established power-law scaling concepts for regime-dependent dynamics.

The unified constitutive model, integrating the Carreau–Yasuda fluid behavior with temperature (TTS) and concentration (TCS) shift factors, is defined as follows:

$$\eta(\dot{\gamma}, T, w_p) = a_c(w_p) \cdot b_c(w_p) \cdot a_T(T) \cdot \eta_0 \left[1 + \left(a_T(T) \cdot a_c(w_p) \cdot \lambda\dot{\gamma}\right)^a\right]^{\frac{n-1}{a}} \tag{6}$$

The proposed model incorporates a total of 10 free parameters: four defining the reference Carreau–Yasuda master curve (η_0, λ, n, a), one for the Arrhenius temperature dependence (E_a), and five characterizing the regime-dependent concentration scaling ($\beta_{c,140}$, $\beta_{c,160}$, $\beta_{c,180}$, β_{conc}, β_{dil}). While the structural Carreau–Yasuda parameters and the flow activation energy remain constant across the entire experimental space, the shift factors explicitly depend on temperature and polymer weight fraction as defined in Equations (2–4).

Given the high dimensionality of the parameter space and the non-linear nature of Equation (6), the error surface is inherently prone to multiple local minima. To ensure the robust identification of the global minimum, a two-step hybrid optimization strategy was employed. Initially, a Particle Swarm Optimization (PSO) algorithm was implemented in Python. This stochastic heuristic method broadly explored the parameter space to identify the region of the global optimum without requiring gradient information. The resulting parameter set then served as the initial guess for a subsequent deterministic optimization utilizing the Generalized Reduced Gradient (GRG) algorithm to precisely converge on the minimum.

The objective function minimized during this iterative process was the mean relative error (MRE) of the predicted viscosity compared to the experimental steady-shear data. By minimizing the relative error rather than the absolute residuals, the fitting routine implicitly accounts for the logarithmic distribution of the viscosity data. This statistical approach ensures equal weighting of the data points across the nine decades of viscosity magnitude, preventing the optimization from being mathematically dominated by the high-viscosity values of the neat polymer melt. The optimized parameters are summarized in Table 1.

Consistent with the theoretical framework delineated in Section 3.3, the concentration scaling is partitioned into two distinct dynamic regimes: the concentrated (entangled) state and the semi-dilute (unentangled) state. Empirical analysis of the rheological data, as depicted for a low shear rate in Figure 9a, identifies the critical transition point between these regimes at

a diluent concentration of approximately 60 m%. Beyond this threshold, the model accounts for the regime change through a distinct increase in the scaling exponent.

The predictive capability of the calibrated model is illustrated in Figure 9b, which depicts the parity between the experimental steady-shear viscosity data and the model predictions. Despite covering a dynamic range spanning over nine decades of viscosity, the global fit achieves a MRE of less than 12%. This confirms that the proposed empirical scaling approach effectively captures the rheological transitions across the investigated temperature and concentration intervals.

To provide a visual reference for the magnitude of the viscosity reduction, the viscosity of the pure diluent is explicitly included in the graphical representation. This comparison illustrates the substantial viscosity disparity spanning several orders of magnitude, extending from the concentrated and semi-dilute regimes down to the pure solvent limit.

However, it is important to note that a rigorous parameterization of the specific crossover from the semi-dilute to the true dilute state, theoretically predicted to occur at polymer concentrations below 5 m%, would require a significantly higher density of experimental measurements in this specific regime to fully resolve the underlying scaling laws.

Figure 10 depicts the steady-shear viscosity profiles of the PE-LD/CS system at the evaluated isotherms. Experimental data are represented by symbols, whereas the model predictions are denoted by solid lines. The progressive influence of dilution is clearly distinct: as the solvent weight fraction increases, the material response transitions from the pronounced shear-thinning behavior characteristic of the entangled melt to a broadly

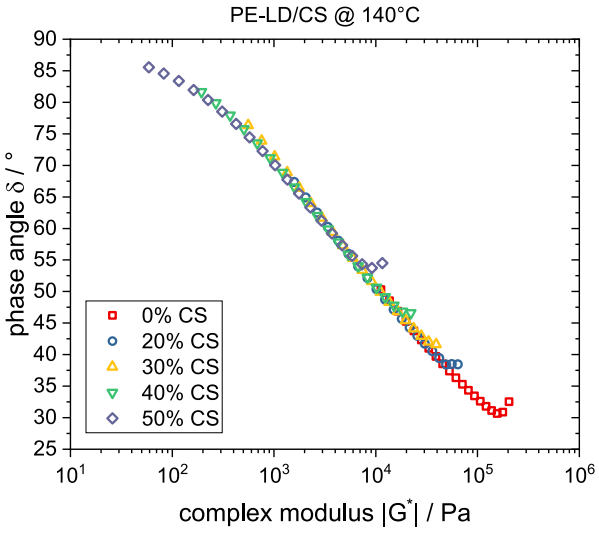

(a) PE-LD/CS at 140 °C

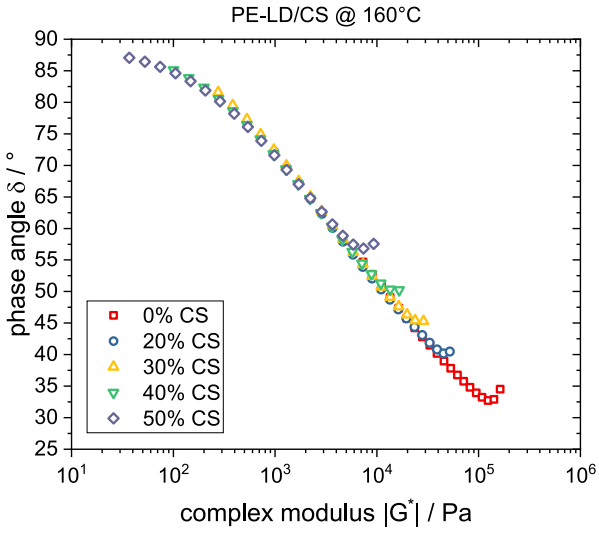

(b) PE-LD/CS at 160 °C

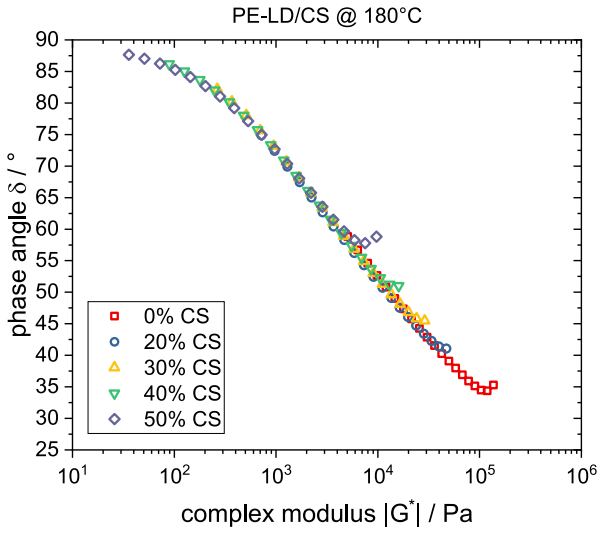

(c) PE-LD/CS at 180 °C

FIGURE 7 | van Gurp–Palmen plots of PE-LD/CS mixtures. The uniform superposition of data points confirms concentration-rheologically simple behavior across the tested isotherms.

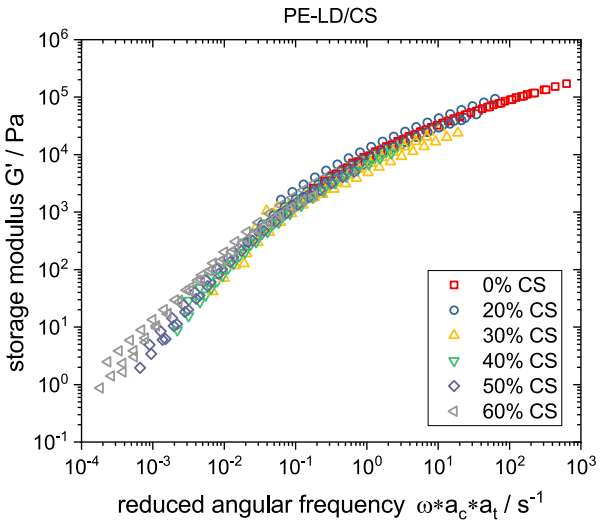

(a) Superposed storage modulus of PE-LD/CS system.

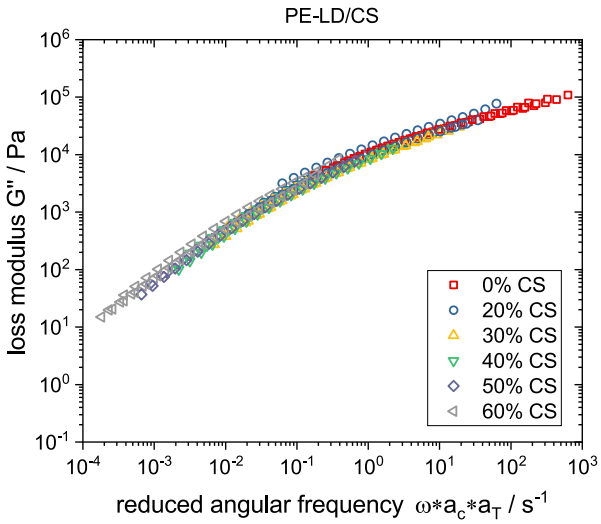

(b) Superposed loss modulus of PE-LD/CS system.

FIGURE 8 | Mastercurves of the storage and loss modulus for all oscillatory measurements shifted to 140°C and 0 m% CS.

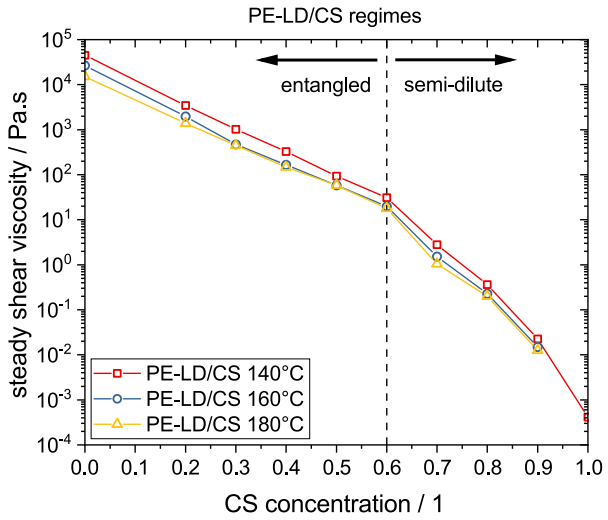

(a) Steady-shear viscosity vs. solvent concentration at the lowest common valid shear rate $\dot{\gamma} = 0.105\,\mathrm{s}^{-1}$

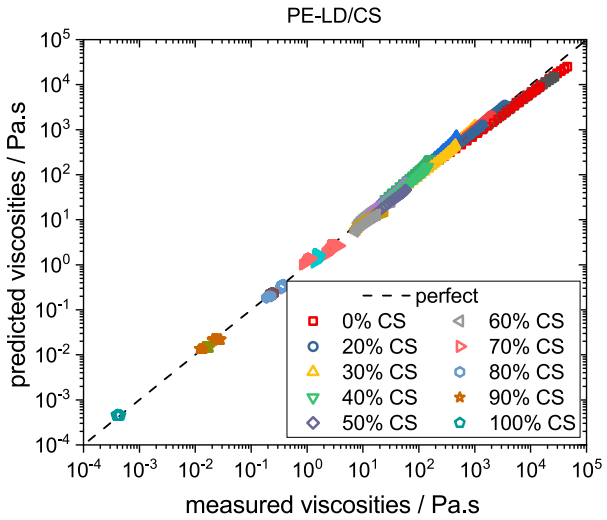

(b) Global scatter plot

FIGURE 9 | Multi-regime viscosity modeling of PE-LD/CS. (a) Transition between concentrated and semi-dilute regimes. (b) Global model validation across all temperatures and concentrations.

defined Newtonian plateau typical of the semi-dilute regime. Concurrently, the onset of non-Newtonian flow systematically shifts toward higher shear rates.

5 | Conclusions

This study successfully established a robust semiempirical modeling framework to predict the shear viscosity of PE-LD diluted with a specialty solvent inherent to the CreaSolv-process. The model encompasses the entire concentration range (0 to 100 m% diluent) and accurately captures the dependencies on temperature, shear rate, and dilution. Despite covering a vast dynamic range of viscosity, spanning from approximately 1×10^{-4} Pa s to 1×10^{5} Pa s, the proposed model demonstrates high predictive fidelity, achieving a MRE of less than 12% across all investigated regimes.

However, certain experimental constraints inherent to the utilized offline characterization methodology must be acknowledged. First, the accessible temperature window was bounded at the upper limit by the onset of solvent volatility and at the lower limit by the rapid increase in viscosity, which imposed handling difficulties during sample loading and stirrer insertion. Consequently, data acquisition for high-viscosity blends (e.g., 10 m% diluent) was precluded by the torque limits of the concentric cylinder geometry. Furthermore, the necessity to combine data from distinct rheological configurations, parallel-plate rheometry for the neat polymer melt versus concentric cylinder geometry for the solutions, introduces a

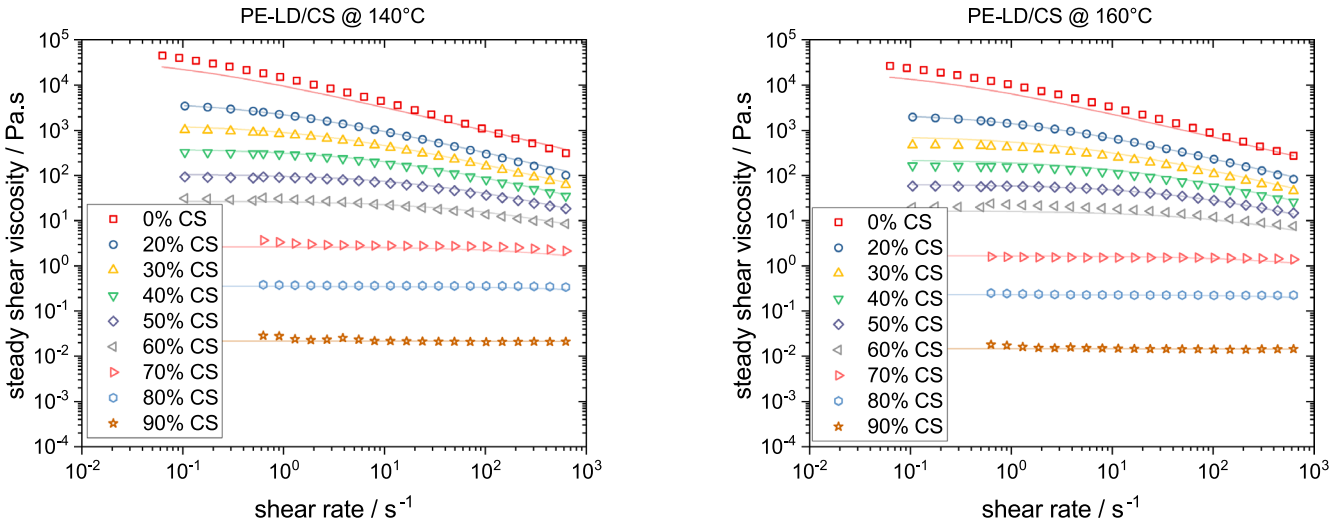

(a) Isotherm at 140 °C.

(b) Isotherm at 160 °C.

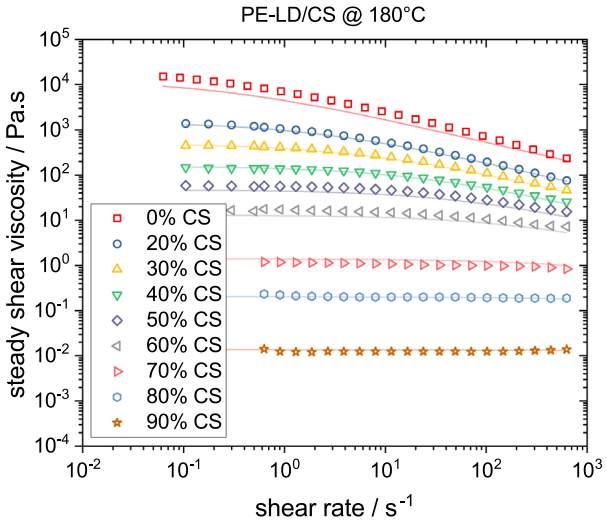

(c) Isotherm at 180 °C.

FIGURE 10 | Steady-shear viscosity of the PE-LD/CS system: Comparison of experimental data (symbols) and model predictions (lines) at varying concentrations for different temperatures (a) 140°C, (b) 160°C, and 180°C.

potential source of experimental uncertainty due to geometric scaling effects.

Additionally, regarding the thermal dependence, theoretical considerations imply that the temperature shift factor (a_T) is not constant but should diminish at higher diluent concentrations. While preliminary experimental data indicated such a dependency, significant experimental variance prevented the formulation of a statistically robust constitutive model to satisfactorily capture this effect. Consequently, this study maintained a global approach for the temperature shift, leaving the detailed parameterization of the concentration-dependent activation energy as a subject for future investigation.

Closely related to this is the observed interplay between thermal expansion (of free volume) and dilution efficiency. It was found that the magnitude of viscosity reduction induced by the diluent is less pronounced at elevated temperatures. Theoretically, this can be attributed to the fact that high temperatures already generate a substantial fractional free volume within the polymer melt; thus, the relative contribution of the solvent-induced free volume becomes less critical compared to the low-temperature state. This physical phenomenon is quantitatively reflected in the model parameters, specifically in the temperature-dependent concentration scaling exponent β_c, which was observed to decrease with increasing temperature.

To circumvent these constraints in future investigations, the implementation of slit rheometry coupled with in-line diluent injection is recommended. As demonstrated in our previous work [37], such a closed-loop configuration effectively mitigates issues related to solvent evaporation and sample handling, thereby enabling precise characterization across a broader spectrum of temperatures and concentrations relevant to industrial

recycling processes. However, it must be noted that while this in-line approach resolves the volatility and viscosity-limit issues of offline rheometry, it introduces distinct boundary conditions. Specifically, the attainable dilution range is often capped by the injection system's capacity; sensitivity of pressure transducers; and the accessible shear rate window may be narrower compared to rotational rheometry, necessitating a careful trade-off between experimental flexibility and process-realistic conditions.

Author Contributions

Johannes Krug: investigation, data curation, methodology, conceptualization. **Ernst Georg Viehböck:** conceptualization, investigation, writing – original draft, methodology, validation, visualization, writing – review and editing, software, formal analysis, data curation, supervision, project administration. **Alexander Hammer:** conceptualization, methodology, writing – review and editing, project administration, supervision, funding acquisition. **Ursula Steiner:** conceptualization, methodology, project administration, supervision, writing – review and editing, funding acquisition. **Christof Murnig:** resources. **Martin Reichel:** resources. **Christian Paulik:** resources, funding acquisition, project administration, supervision. **Gerald Berger-Weber:** resources, writing – review and editing, funding acquisition, project administration, supervision.

Acknowledgments

During the preparation of this work, the authors used Chat GPT-5 and Gemini 3 Pro in order to increase readability and image generation. After using this tool, the authors reviewed and edited the content as needed and take full responsibility for the content of the published article. Open Access funding provided by Johannes Kepler Universitat Linz/KEMÖ.

Funding

The authors gratefully acknowledge financial support through the FTI initiative circular economy project "circPLAST-mr" (funding number 889843). Furthermore, this work was conducted within the framework of the COMET—Competence Centers for Excellent Technologies program, supported by the COMET Center CHASE and the COMET Center Pro2Future (Contract No. 911655). The COMET program is funded by the Austrian Federal Ministry for Innovation, Mobility and Infrastructure (BMIMI), the Austrian Federal Ministry for Economy, Energy and Tourism (BMWET), and the Federal Provinces of Upper Austria, Vienna, and Styria. The COMET program is managed by the Austrian Research Promotion Agency (FFG). Open access funding was provided by the Johannes Kepler University Open Access Publishing Fund and the Federal State of Upper Austria.

Conflicts of Interest

The authors declare no conflicts of interest.

Data Availability Statement

The data that support the findings of this study are available from the corresponding author upon reasonable request.

References

1. S. L. Nordahl, N. R. Baral, B. A. Helms, and C. D. Scown, "Complementary Roles for Mechanical and Solvent-Based Recycling in Low-Carbon, Circular Polypropylene," *Proceedings of the National Academy of Sciences of the United States of America* 120, no. 46 (2023): e2306902120, https://doi.org/10.1073/pnas.2306902120.

2. T. Giulia, M. Cristiano, A. Stefano, O. M. Aldo, and P. Carlo, "Nylon Recycling Processes: A Brief Overview," *Chemical Engineering Transactions* 100 (2023): 727–732, https://doi.org/10.3303/CET23100122.

3. Z. Tadmor and I. Klein, *Engineering Principles of Plasticating Extrusion* (R.E. Krieger, 1985) OCLC: 19080909.

4. M. Doi and S. F. Edwards, *The Theory of Polymer Dynamics. No. 73 in International Series of Monographs on Physics*, Reprint ed. (Clarendon Press, 1994).

5. L. J. Gerhardt, C. W. Manke, and E. Gulari, "Rheology of Polydimethylsiloxane Swollen With Supercritical Carbon Dioxide," *Journal of Polymer Science Part B: Polymer Physics* 35, no. 3 (1997): 523–534, https://doi.org/10.1002/(SICI)1099-0488(199702)35:3<523::AID-POLB11>3.0.CO;2-J.

6. Y. Heo and R. G. Larson, "The Scaling of Zero-Shear Viscosities of Semidilute Polymer Solutions With Concentration," *Journal of Rheology* 49, no. 5 (2005): 1117–1128, https://doi.org/10.1122/1.1993595.

7. C. Q. Li, H. H. Winter, Y. Q. Fan, G. X. Xu, and X. F. Yuan, "Time–Concentration Superposition for Linear Viscoelasticity of Polymer Solutions," *Polymers* 15, no. 7 (2023): 1807, https://doi.org/10.3390/polym15071807.

8. J. D. Ferry, *Viscoelastic Properties of Polymers* (John Wiley & Sons, 1980).

9. A. Schausberger, H. Knoglinger, and H. Janeschitz-Kriegl, "The Role of Short Chain Molecules for the Rheology of Polystyrene Melts. II. Linear Viscoelastic Properties," *Rheologica Acta* 26 (1987): 468–473.

10. H. Knoglinger, A. Schausberger, and H. Janeschitz-Krieg, "The Role of Short Chain Molecules for the Rheology of Polystyrene Melts. I. Molar Mass Dependent Shift Factors," *Rheologica Acta* 26 (1987): 460–467.

11. G. Gschwendner, "Viscoelastic Behavior of Diluted Polyethylene" (master thesis, 2024).

12. A. Schausberger and I. V. Ahrer, "On the Time-Concentration Superposition of the Linear Viscoelastic Properties of Plasticized Polystyrene Melts Using the Free Volume Concept," *Macromolecular Chemistry and Physics* 196, no. 7 (1995): 2161–2172, https://doi.org/10.1002/macp.1995.021960707.

13. L. J. Gerhardt, A. Garg, C. W. Manke, and E. Gulari, "Concentration-Dependent Viscoelastic Scaling Models for Polydimethysiloxane Melts With Dissolved Carbon Dioxide," *Journal of Polymer Science Part B: Polymer Physics* 36, no. 11 (1998): 1911–1918, https://doi.org/10.1002/(SICI)1099-0488(199808)36:11<1911::AID-POLB12>3.0.CO;2-A.

14. J. R. Royer, Y. J. Gay, J. M. Desimone, and S. A. Khan, "High-Pressure Rheology of Polystyrene Melts Plasticized With CO_2: Experimental Measurement and Predictive Scaling Relationships," *Journal of Polymer Science Part B: Polymer Physics* 38, no. 23 (2000): 3168–3180, https://doi.org/10.1002/1099-0488(20001201)38:23<3168::AID-POLB170>3.0.CO;2-E.

15. J. M. Dealy and J. Wang, *Melt Rheology and Its Applications in the Plastics Industry. Engineering Materials and Processes* (Springer Netherlands, 2013).

16. H. Park and J. Dealy, "Effects of Pressure and Supercritical Fluids on the Viscosity of Polyethylene," *Macromolecules* 39 (2006): 5438–5452, https://doi.org/10.1021/ma060735+.

17. E. G. Viehböck, A. Hammer, C. Paulik, and G. Berger-Weber, "Viscosity Reduction in Diluted Polyethylene Melts: A Comparative Study of Semi-Empirical, Viscoelastic, and Equation-of-State Modeling Frameworks," 2026.

18. T. Mezger, *Das Rheologie Handbuch: Für Anwender von Rotations- und Oszillations-Rheometern*, 5, vollständig überarbeitete auflage ed. (Farbe und Lack Bibliothek: Vincentz Network, 2016).

19. A. Yoshimura and R. K. Prud'homme, "Wall Slip Corrections for Couette and Parallel Disk Viscometers," *Journal of Rheology* 32, no. 1 (1988): 53–67, https://doi.org/10.1122/1.549963.

20. P. J. Carreau, "Rheological Equations From Molecular Network Theories" (PhD thesis, University of Wisconsin, 1968).

21. K. Yasuda, R. C. Armstrong, and R. E. Cohen, "Shear Flow Properties of Concentrated Solutions of Linear and Star Branched Polystyrenes," *Rheologica Acta* 20 (1981): 163–178.

22. C. W. Macosko, ed., *Rheology: Principles, Measurements, and Applications*. Advances in Interfacial Engineering Series, (VCH, 1994).

23. T. A. Osswald and N. S. Rudolph, *Polymer Rheology: Fundamentals and Applications* (Hanser Publications, 2015).

24. M. L. Williams, R. F. Landel, and J. D. Ferry, "The Temperature Dependence of Relaxation Mechanisms in Amorphous Polymers and Other Glass-Forming Liquids," *Journal of the American Chemical Society* 77, no. 14 (1955): 3701–3707, https://doi.org/10.1021/ja01619a008.

25. T. Schaible and C. Bonten, "In-Line Measurement and Modeling of Temperature, Pressure, and Blowing Agent Dependent Viscosity of Polymer Melts," *Applied Rheology* 32, no. 1 (2022): 69–82, https://doi.org/10.1515/arh-2022-0123.

26. S. Banik, D. Kong, M. J. San Francisco, and G. B. McKenna, "Monodisperse Lambda DNA as a Model to Conventional Polymers: A Concentration-Dependent Scaling of the Rheological Properties," *Macromolecules* 54, no. 18 (2021): 8632–8654, https://doi.org/10.1021/acs.macromol.0c02537.

27. J. Langwieser, "Process Insights and Strategies for Quality Enhancement in Plastic Film Recycling" (PhD thesis, Johannes Kepler Universität Linz, 2025).

28. E. Kastner, *Zeit-Konzentration-Superposition am Beispiel konzentrierter Polyethylenlösungen* (Johannes Kepler Universität Linz, 1996).

29. C. Kwag, "Rheology of Molten Polystyrene With Dissolved Gases" (PhD thesis, Wayne State University, 1998).

30. J. D. J. Rathinaraj, B. Keshavarz, and G. H. McKinley, "Why the Cox–Merz Rule and Gleissle Mirror Relation Work: A Quantitative Analysis Using the Wagner Integral Framework With a Fractional Maxwell Kernel," *Physics of Fluids* 34, no. 3 (2022): 033106, https://doi.org/10.1063/5.0084478.

31. W. P. Cox and E. H. Merz, "Correlation of Dynamic and Steady Flow Viscosities," *Journal of Polymer Science* 28, no. 118 (1958): 619–622, https://doi.org/10.1002/pol.1958.1202811812.

32. B. L. Walter, J. P. Pelteret, J. Kaschta, D. W. Schubert, and P. Steinmann, "On the Wall Slip Phenomenon of Elastomers in Oscillatory Shear Measurements Using Parallel-Plate Rotational Rheometry: I. Detecting Wall Slip," *Polymer Testing* 61 (2017): 430–440, https://doi.org/10.1016/j.polymertesting.2017.05.035.

33. N. S. Akkarachittoor, A. L. Fricke, and J. D. Small, "Dual Chamber Capillary Viscometer for Viscosity Measurements of Concentrated Polymer Solutions at Elevated Temperatures," *Review of Scientific Instruments* 57, no. 6 (1986): 1182–1184, https://doi.org/10.1063/1.1138626.

34. R. A. Mendelson, "A Method for Viscosity Measurements of Concentrated Polymer Solutions in Volatile Solvents at Elevated Temperatures," *Journal of Rheology* 23, no. 5 (1979): 545–556, https://doi.org/10.1122/1.549509.

35. H. E. Park and J. M. Dealy, "Effects of Supercritical Fluids, Pressure, Temperature, and Molecular Structure on the Rheological Properties of Molten Polymers," *AIP Conference Proceedings* 1027, no. 1 (2008): 366–368, https://doi.org/10.1063/1.2964693.

36. C. I. Chung, *Extrusion of Polymers: Theory and Practice* (Carl Hanser Verlag GmbH & Co. KG, 2019).

37. E. G. Viehböck, A. Hammer, M. Kirchmayr, C. Murnig, C. Paulik, and G. Berger-Weber, "Slit-Rheometry-Based Characterization of the Flow Behavior of Diluted Polymer Melts," *Journal of Rheology* 70, no. 1 (2026): 35–45, https://doi.org/10.1122/8.0001059.